Transmission Electron Microscopy

Part VII: Analytical Electron Microscopy (AEM)
EELS & EDXS

Christoph T. Koch

Max Planck Institut für Metallforschung

Literature:R.F. Edgerton, *Electron Energy-Loss Spectroscopy in the Electron Microscope,*Plenum, New York (1986, 1996)

Reminder: Electron Scattering in the Sample

Electrons incident on the sample may be deflected and/or transfer part of their energy to the sample.

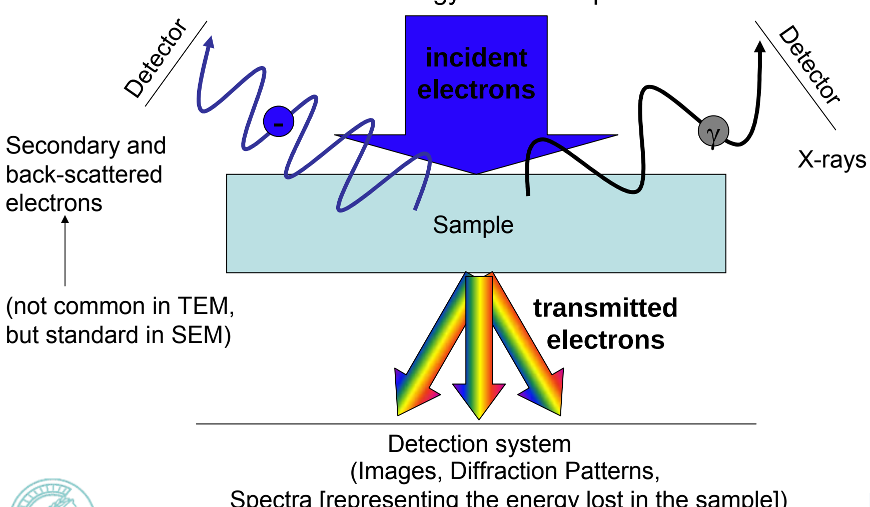

"An artist's view" of electron scattering

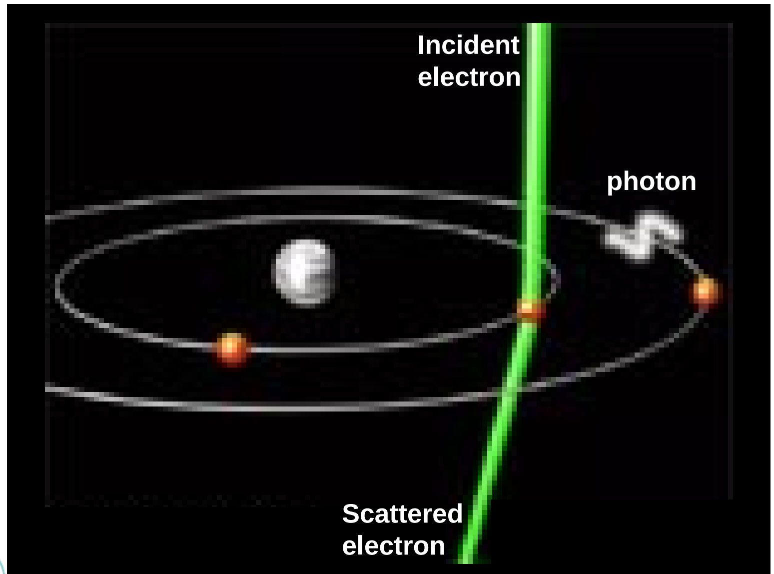

Image and animation: Carl Zeiss SMT

Reminder: Inelastic Scattering

Electrons may lose energy by

- Exciting vibrational states (phonons) in the sample ($\Delta E < 0.2eV$)
- Exciting density fluctuations of electrons in the valence band (surface- and bulk plasmons) ($5\ eV < \Delta E < 50\ eV$)
- Exciting bound electrons into an unoccupied orbital (LUMO or higher)
- Inter- and Intra band transitions
- Producing Bremsstrahlung
- Electron – electron (Compton) scattering

Separating Electrons by Energy

Slower electrons experience a stronger deflection by the magnetic field.
The momentum p of the electron may then be determined from the **radius of curvature a**:

$$p = \frac{e}{c}\left|\vec{B}_\perp\right| a, \qquad \left(E = \frac{p^2}{2m}\right)$$

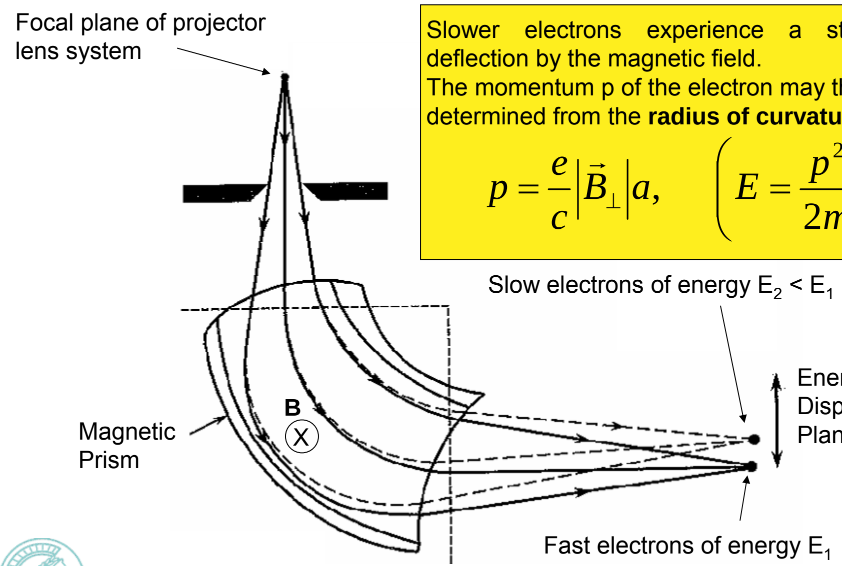

The Electron Energy Loss Spectrum

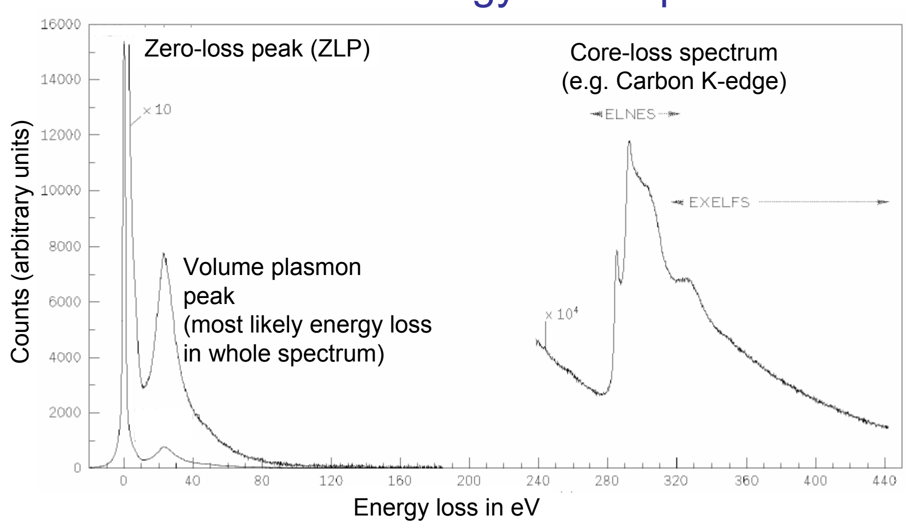

ELNES: electron energy near edge structure
EXELFS: Extended energy loss fine structure

Origin of EELS Core-Loss Features

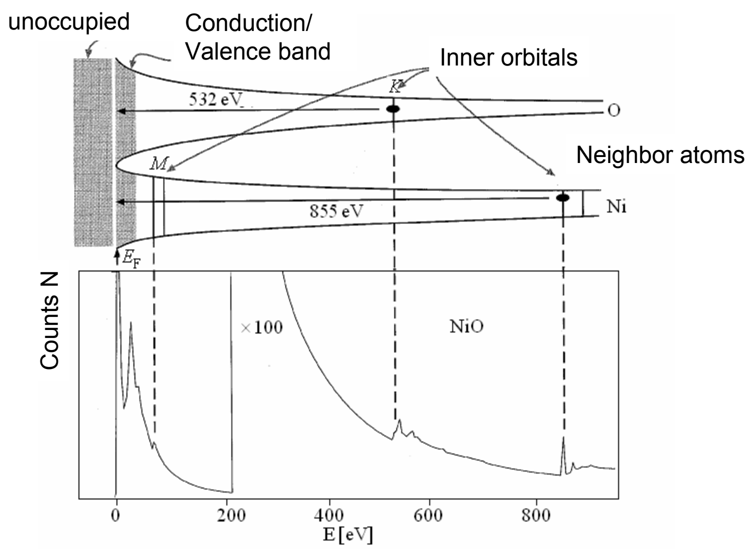

Naming Convention for Atomic Orbitals (Electron Shells)

Electronic excitations visible in the energy loss spectrum are named after the shell from which an electron was excited.

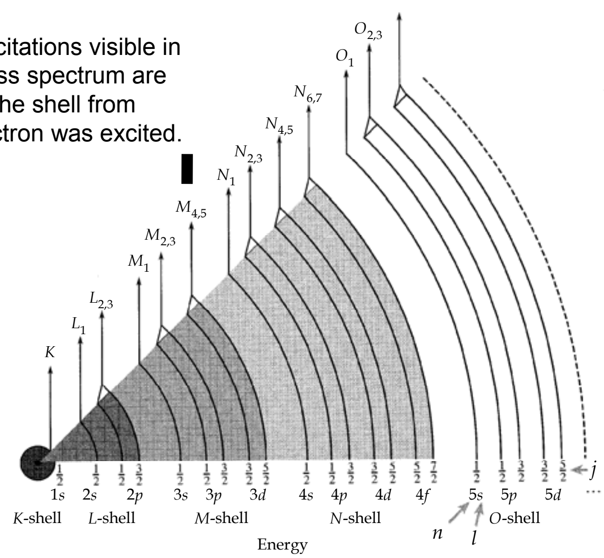

Example: EEL Spectrum of Boron Nitride

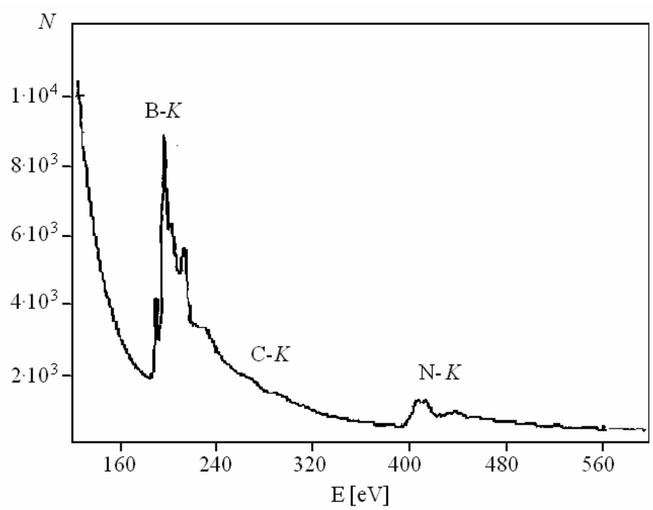

EEL spectrum of Boron Nitride

Inelastic Scattering Geometry

Ewald sphere radius: k_0
Beam energy: E_0

$$E_0 = \frac{p^2}{2m} = \frac{h^2 |\vec{k}_0|^2}{2m}$$

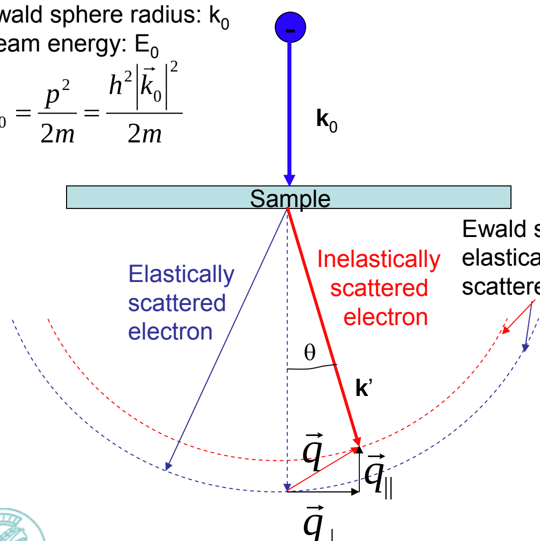

$$\vec{q} = \vec{k}' - \vec{k}_0$$

$$\vec{q} = \vec{q}_{||} + \vec{q}_{\perp}$$

$$|\vec{q}_{\perp}| \approx \vartheta\, |\vec{k}_0|, \quad |\vec{q}_{||}| \approx \vartheta_E |\vec{k}_0|$$

$$|\vec{q}|^2 \approx |\vec{k}_0|^2 \left(\vartheta^2 + \vartheta_E{}^2\right)$$

$$\vartheta_E = \Delta E / \left(\gamma m_0 v^2\right)$$

Angular Dependence of Inelastic Scattering

Characteristic Angle: $\bar{\vartheta}_E = \bar{E} / 2E_0$ ($\bar{E}$ = average energy loss, typically 37eV)

Differential cross section for inelastic scattering:

$$\frac{d\sigma}{d\Omega} = \frac{4\gamma^2 Z}{a_0^2 k_0^4} \frac{1}{\left(\vartheta^2 + \bar{\vartheta}_E^2\right)^2} \left\{1 + \frac{\vartheta_0^4}{\left(\vartheta^2 + \vartheta_E^2 + \vartheta_0^2\right)^2}\right\} \propto \begin{cases} \vartheta^0, \text{ for } \vartheta < \vartheta_E \\ \vartheta^{-2}, \text{ for } \vartheta_E < \vartheta < \vartheta_0 \\ \vartheta^{-4}, \text{ for } \vartheta_0 < \vartheta \end{cases}$$

Compare: Elastic Rutherford scattering cross section is proportional Z^2!

a_0: Bohr radius (=0.529Å)
γ: relativistic correction factor
θ: scattering angle
θ_0: effective cutoff angle
θ_E: characteristic angle

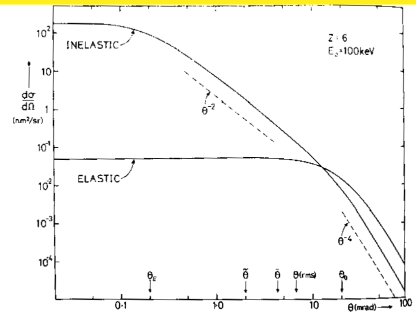

Bethe Theory and Dipole Approximation

Scattering cross section for an electron from the initial state |i> into a state |n> :

$$\frac{d\sigma_n}{d\Omega} = \left(\frac{4\gamma^2}{a_0^2 q^4}\right) \frac{k'}{k_0} \left| \left\langle n \left| \sum_j \exp(i\vec{q}\cdot\vec{r}_j) \right| i \right\rangle \right|^2$$

$$= \left(\frac{4\gamma^2}{a_0^2 q^4}\right) \frac{k'}{k_0} \left| \int \Psi_f^*(r) \sum_j \exp(i\vec{q}\cdot\vec{r}_j) \Psi_i(\vec{r}) d^3 r \right|^2$$

|n>: Target electron orbital
|i>: Initial electron orbital
q: Scattering vector
r_j: Atom positions

Dipole approximation: $\exp(i\vec{q}\cdot\vec{r}_j) = 1 + i\vec{q}\cdot\vec{r} - \ldots$
(for orbitals close to the core only the local atom at r=0 must be considered)

$$\Rightarrow \left|\left\langle n \middle| \exp(i\vec{q}\cdot\vec{r}) \middle| i \right\rangle\right|^2 = \left|\left\langle n \middle| 1 \middle| i \right\rangle + i\left\langle n \middle| \vec{q}\cdot\vec{r} \middle| i \right\rangle - \ldots\right|^2 = \left| i\left\langle n \middle| \vec{q}\cdot\vec{r} \middle| i \right\rangle - \ldots\right|^2$$

Vanishes, because |Ψi> and |Ψn> are orthogonal

Non-zero only for pairs of states |i> and |n> whose symmetry is different, i.e. whose angular momentum changes.

Dipole Selection Rule: Change in angular momentum Δl = +/-1

Physical Significance of Matrix Element

$$M(\vec{q},E) = \left|\langle n|\exp(i\vec{q}\cdot\vec{r})|i\rangle\right|^2 \approx \left|i\langle n|\vec{q}\cdot\vec{r}\,|i\rangle\right|^2$$

- The matrix element determines the **basic edge shape**. ELNES and EXELFS oscillations modify this shape.
- Computation of the basic edge shapes only requires isolated atoms.

1. Basic edge for isolated atom

2. Spectrum containing background (e.g. from other edges)

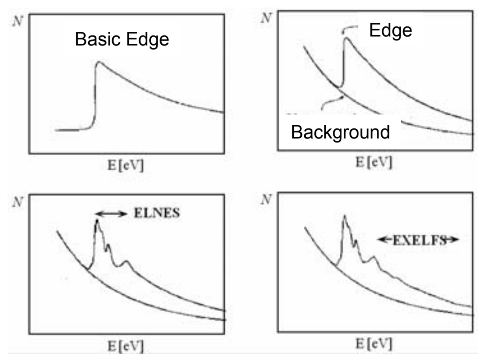

3. Modulation by fine structure

4. Modulation by far-edge-fine structure

Energy Loss Near Edge Structure (ELNES)

ELNES provides information about local band structure, oxidation states and bonding. Its computation requires therefore (time consuming) band structure computations or equivalent methods in real space.

• The ELNES Signal may be interpreted as the local symmetry-projecteddensity of states in the conduction band

• Core-hole effect: The electron that has been excited into one of the unoccupied atomic orbitals leaves behind a hole, producing a shift on all the other orbitals, including the one it is jumping to. This affects the ELNES.

• One can often distinguish local bonding characteristics by Fingerprinting, i.e. by comparing with spectra of the same element in known local environments.

EXtended Energy-Loss Fine Structure (EXELFS)

If a core-shell electron is excited enough to leave the potential of ist local atom it travels through the sample as a spherical wave. The inteference of this outgoing wave with the ones reflected by neighboring atoms affects the ionization probability, modulating the ionization edge structure (see also X-ray technique EXAFS).

- EXELFS carries information about the coordination of an atomic species in a material.
- It starts at energies $>E_c+50$ eV (E_c = edge energy)
- It may be overlaid by multiple scattering effects (e.g. E_c + plasmon loss) => Single scattering correction (deconvolution with low-loss EEL spectrum) is necessary.
- Radial distribution function (RDF) may be obtained from EXELFS.

Low-Loss EELS

- Mainly Plasmons (longitudinal density fluctuations in a plasma, here: the electrons in the valence band)
- Also Intra- and Interband transitions (as opposed to ionization edges, which catapult electrons into the conduction band or outside the local atom's potential).
- Energy loss range comparable with the range accessible to V-UV spectroscopy.
- Information about (local) dielectric properties of the material: Determination of dielectric function with high spatial resolution

$$\varepsilon = \varepsilon_r + i\varepsilon_i = \varepsilon_1 + i\varepsilon_2$$

- Excitation / annihilation of atomic vibrations (phonons): Energy losses << 1eV.

Dielectric Formulation of Energy Loss

The dielectric formulation of energy losses considers a continuum of varying (complex) dielectric constant, instead of individual atomic orbitals.

Double differential cross section ($q^2 = k_0^2\left(\theta^2 + \theta_E^2\right)$)

$$\frac{d^2\sigma}{dEd\Omega} = \frac{const}{q^2} Im\left(-\frac{1}{\varepsilon(E,q)} \right) = \frac{const}{\theta^2 + \theta_E^2} Im\left(-\frac{1}{\varepsilon(E,q)} \right)$$

Kramers Kronig Relation relates real and imaginary part of the dielectric function. The full complex $\varepsilon = \varepsilon_1 + i\varepsilon_2$ can therefore be obtained from a single EEL spectrum $(E = \hbar\omega)$

$$Re\left(\frac{1}{\varepsilon(\omega)}\right) - 1 = \frac{1}{\pi} \, P \int_{-\infty}^{\infty} Im\left(\frac{1}{\varepsilon(\omega')}\right) \frac{1}{\omega' - \omega} d\omega'$$

$$\boxed{\varepsilon_1 = \frac{Re\left(\frac{1}{\varepsilon}\right)}{\left(Re\left(\frac{1}{\varepsilon}\right)\right)^2 + \left(Im\left(\frac{1}{\varepsilon}\right)\right)^2} \qquad \varepsilon_2 = \frac{Im\left(\frac{1}{\varepsilon}\right)}{\left(Re\left(\frac{1}{\varepsilon}\right)\right)^2 + \left(Im\left(\frac{1}{\varepsilon}\right)\right)^2}}$$

Max-Planck Institut für Metallforschung Page: 17 Universität Stuttgart

Models of the Dielectric Function

<u>Drude Model</u>: Valid for Metals and Semiconductors. Assumes the existence of a single plasmon resonance frequency ω_p and a damping coefficient τ (small for metals). ω_p depends on the valence electron density n_e and the effective electron mass m.

$$\varepsilon(\omega) = \varepsilon_1 + i\varepsilon_2 = 1 - \frac{\omega_p^2}{\omega^2 + 1/\tau^2} + \frac{i 1/\tau \, \omega_p^2}{\omega(\omega^2 + 1/\tau^2)} \qquad \omega_p = \left(\frac{n e^2}{\varepsilon_0 m}\right)^{\frac{1}{2}}$$

<u>Lorentz Model</u>: Assumes an ensemble of many different harmonic oscillators representing possible interband transitions with energies equal to the oscillators eigenfrequency ω_n. Commonly only one such harmonic oscillator is assumed:

$$\varepsilon_n = 1 + \frac{n e^2}{m \, \varepsilon_0} \frac{1}{\omega_n^2 - \omega^2 + i\frac{\omega}{\tau}}$$

Max-Planck Institut für Metallforschung Page: 18 Universität Stuttgart

Multiple Inelastic Scattering

Single scattering spectrum (as measured):

$$J^1(E) = R(E) \otimes S(E) = \int_{-\infty}^{\infty} R(E-E')S(E')dE'$$

Instrumental broadening (point spread function)

Actual energy loss function of sample

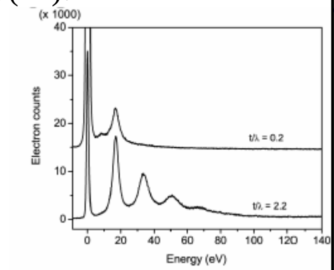

Double scattered spectrum (as detected):

$$J^2(E) = \frac{1}{2I_0} R(E) \otimes S(E) \otimes S(E)$$

Fourier transform of spectrum containing all multiple scattering orders:

$$j(\nu) = \int_{-\infty}^{\infty} J(E) e^{2\pi i \nu E} dE$$

$$j(\nu) = z(\nu)\left(1 + \frac{s(\nu)}{I_0} + \frac{[s(\nu)]^2}{2I_0^2} + \ldots\right) = z(\nu) e^{s(\nu)/I_0}$$

(I_0 = total current in spectrum, z(ν):FT of zero-loss peak shape)

Fourier-Log Deconvolution

If the whole spectrum starting at E=0 is available (possible for low energy losses):

$$s(\nu) = I_0 \ln\left(\frac{j(\nu)}{z(\nu)}\right)$$

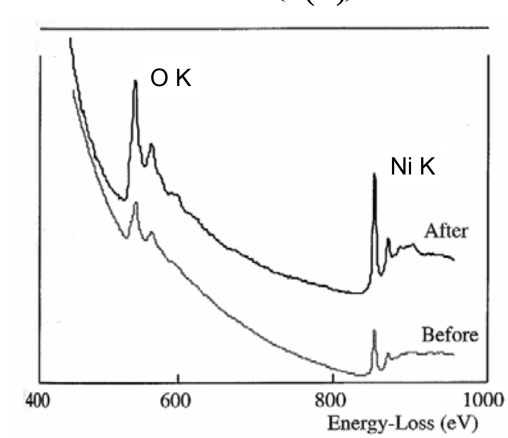

Fourier-Ratio Method

One can approximate the multiple scattering at higher energy losses as a convolution of the actual spectrum with its low-loss range (since low energy losses (e.g. plasmons) have a much higher scattering cross section).
The single scattering energy loss function can then be obtained by deconvolution, using an iterative algorithm (such as Maximum Likelihood, Richardson-Lucy, etc.) or straight division in Fourier-space.

$$k^1(\nu) = I_0 \frac{j_K(\nu)}{j_l(\nu)}$$

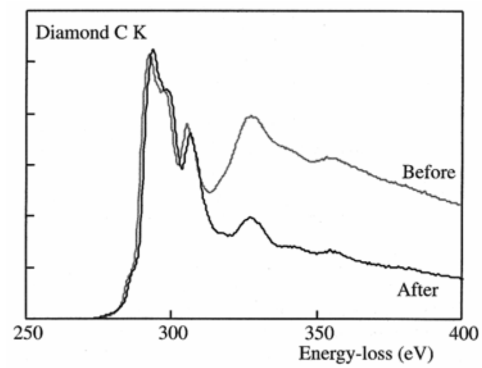

Thickness Determination by EELS

At sufficiently high specimen thickness, several inelastic scattering events may occur. The EELS intensity is then given by an exponential in reciprocal space

$$t/\lambda = \ln\left(I_{total}/I_{ZLP}\right)$$

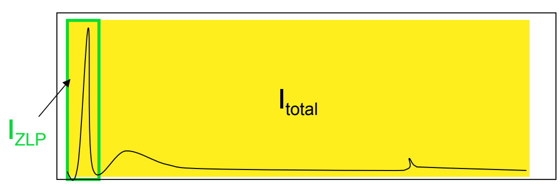

Inelastic Mean Free Path: $\lambda \approx \dfrac{106 \dfrac{1+E_0/1022}{(1+E_0/511)^2} \dfrac{E_0}{E_m}}{\ln\left[2\beta E_0/E_m\right]}$ (E_0 in keV, β=collection angle)

Mean energy loss (in eV): $E_m \approx 7.6 Z^{0.36}$

λ is typically 50 – 150 nm

Delocalization of Inelastic Scattering

At higher Energy losses θ_E becomes larger ($\theta_E \sim E$). For high energy losses the spatial resolution is therefore determined by the size of the spectrometer collection aperture (uncertainty principle).

At low energy losses, qE determines a lower cut-off angle below which the scattering cross section is reduced. It therefore needs to be considered in addition to the aperture size.

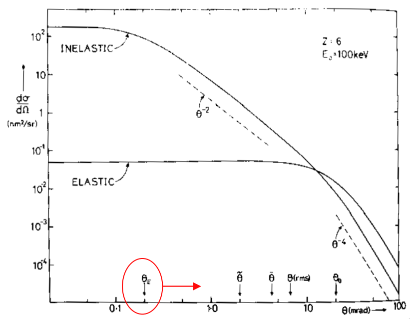

Generally the resolution of inelastic scattering may be approximated by the a disk of diameter d_{50} from which 50% of the inelastic signal stem:

$$(d_{50})^2 = \left(0.5\lambda / \vartheta_E^{3/4}\right)^2 + \left(0.6\lambda / \beta\right)^2$$

Limits low-loss resolution   Raileigh criterion for collection aperture

Delocalization of Inelastic Scattering

Data: Lin Gu, MPI-MF
Microscope: Zeiss Libra 200FE+MC

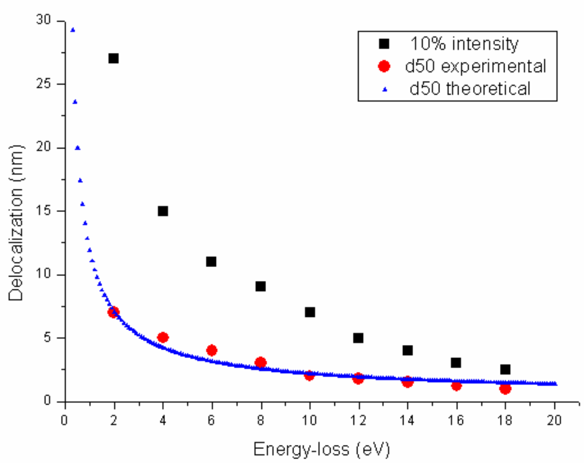

Spatial-resolution of inelastic scattering (neglecting aberrations) using an AlGaN edge (effective CCD pixel size: 2Å). d_{50} experimental reflects an average value with energy-slit of about 2eV.

Separating Electrons by Energy

Focal plane of projector lens system

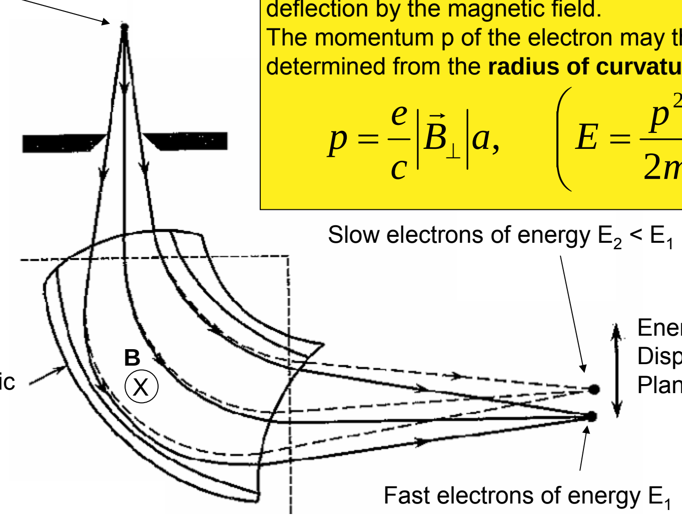

Magnetic Prism

Slower electrons experience a stronger deflection by the magnetic field.
The momentum p of the electron may then be determined from the **radius of curvature a**:

$$p = \frac{e}{c}\left|\vec{B}_{\perp}\right| a, \qquad \left(E = \frac{p^2}{2m} \right)$$

Slow electrons of energy $E_2 < E_1$

Energy Dispersive Plane

Fast electrons of energy E_1

Imaging Energy Filters

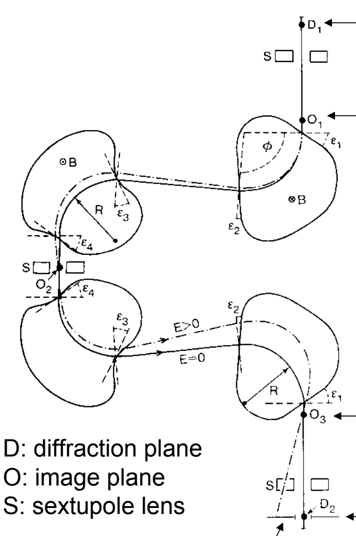

Intermediate Diffraction Pattern

Intermediate Image

Imaging Energy Filter

An optical element (i.e. may have some magnification) which replicates the image in O_1 in O_3, but electrons of different energy cross the image plane O_3 at different angles of incidence.

Achromatic image

Energy dispersed diffraction pattern

D: diffraction plane
O: image plane
S: sextupole lens

Energy-selecting slit aperture

Energy Filter Aberrations

Imaging energy filter aberrations
- Reduce spectral resolution (by convoluting diffraction pattern or image with the spectrum)
- Reduce the area that can be imaged (depends on width of energy-selecting slit).

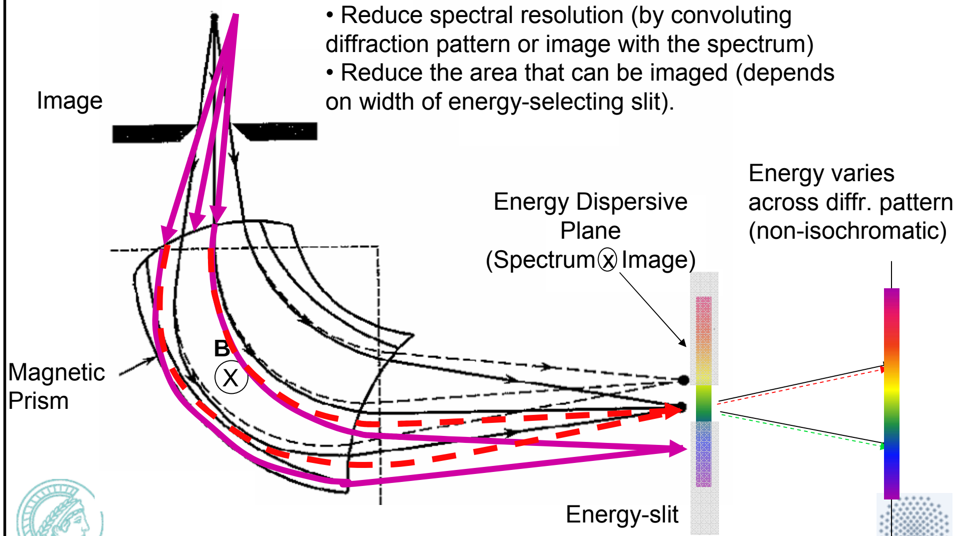

Energy-filtered Electron Diffraction

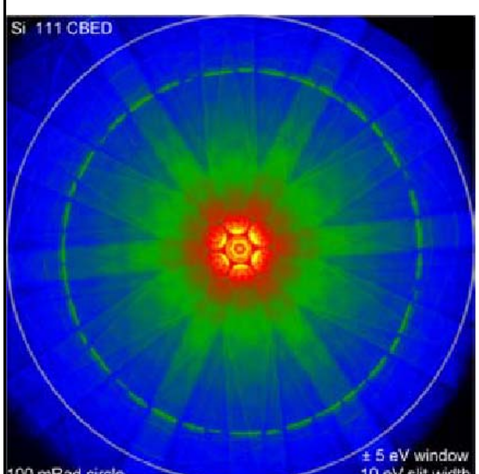

Energy-filtered CBED pattern
(Slit width: 10eV)

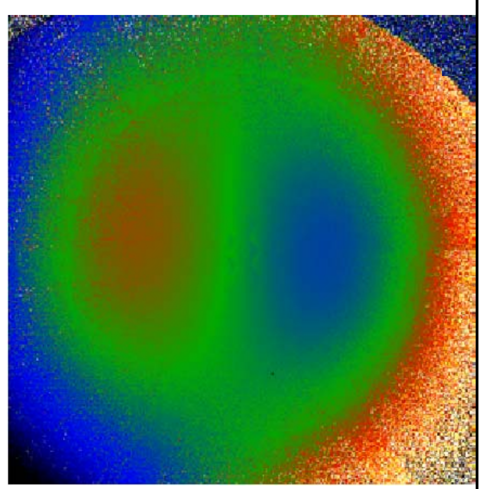

Energy variation for CBED pattern
(Energy loss: 0eV [red] .. 10eV [blue])

(M.M.G. Barfels, M. Kundmann, C. Trevor, J.A. Hunt, Microsc Microanal 11(Suppl 2), 2005)

Correcting Imaging Energy Filter Aberrations

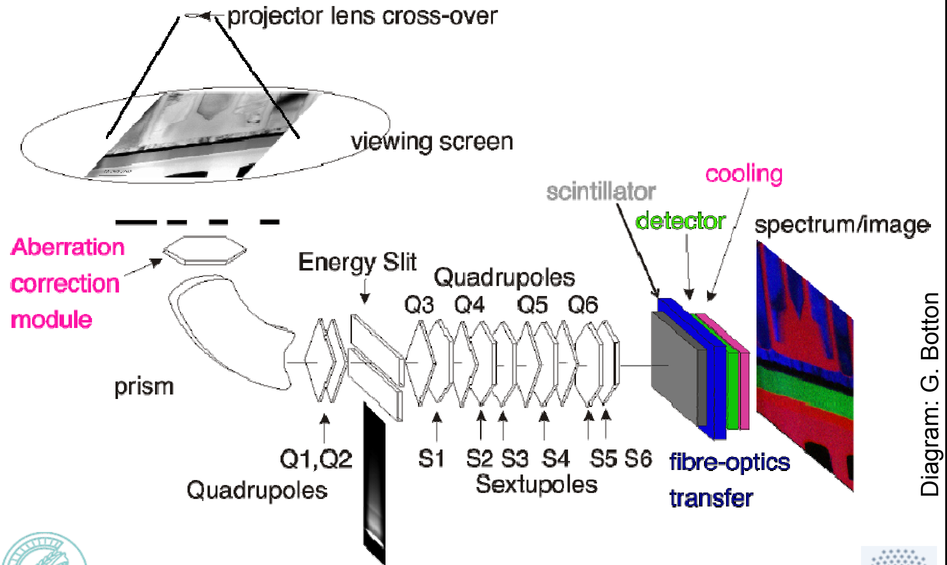

Actual Design of a Post-Column Filter

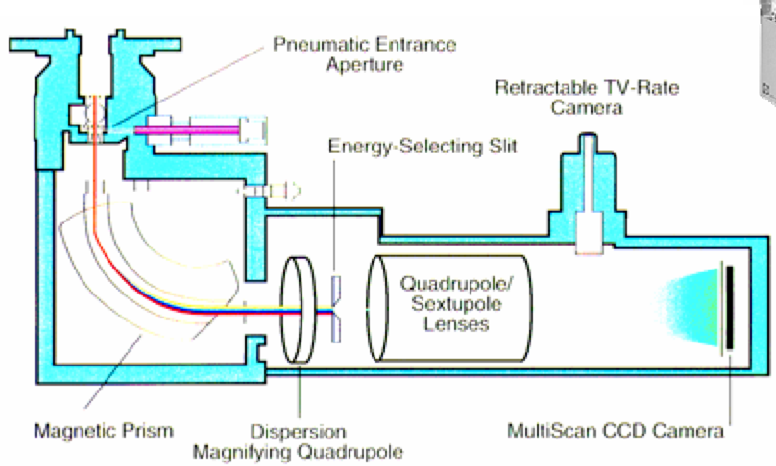

Gatan Imaging Filter (GIF): mounted below the column

In-Column (Omega) Filter

Image and animation: Carl Zeiss SMT

Evolution of In-Column Filter Designs

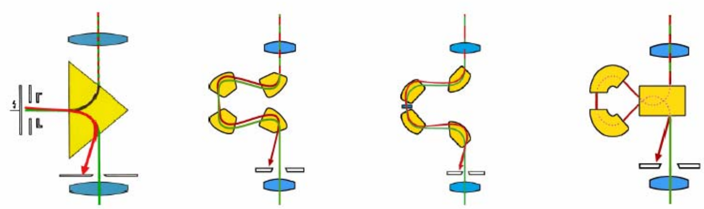

Filter Type	Prism filter	OMEGA filter	corrected OMEGA	Mandoline filter
Instruments	EM 902	LEO 912,LIBRA 120	**LIBRA 200 / SATEM**	SESAM
High tension	80 kV	200 kV	**200 kV**	200 kV
Dispersion	1.5 µm/eV	0.75 µm/eV	**1.85 µm/eV**	6.2 µm/eV
Error Correction	none	2nd order optimized	**2nd order corrected 3rd order optimized**	2nd order corrected 3rd order corrected
Non-Isochromacy (energy shift across negative)	23eV	15eV	0.5eV	0.007eV
Transmissivity („acceptance")	$12nm^2$ 1eV, 80kV	$9nm^2$ 1eV, 200kV	$190nm^2$ 1eV, 200kV	$11000nm^2$ 1eV, 200kV

In-Column vs. Post-Column

In-Column (Omega) Filter

- 4 Dispersive elements (4x90°)
- Integrated into microscope column
- Electron Optics designed to optimize filter performance
- Spectra and images projected on viewing screen, CCD, photographic film, TV-camera

Post-Column Filter

- 1 dispersive element (90°)
- May be added to any existing microscope
- Filter- and microscope optics separately controlled
- Only detectors integrated into energy filter possible (no film, no viewing screen)

Energy-Filtered TEM (EFTEM)

In EFTEM mode, the energy filter is used to record images formed by electrons that have experienced different energy losses.

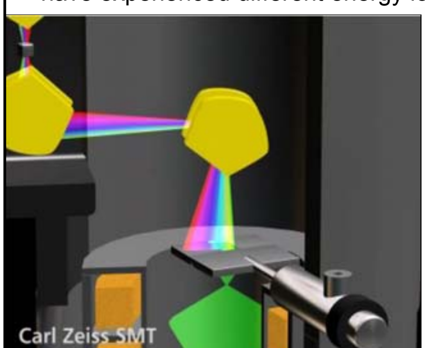

The energy window is shifted by changing the accelerating voltage of the microscope. This ensures that the TEM optics may remain unchanged.

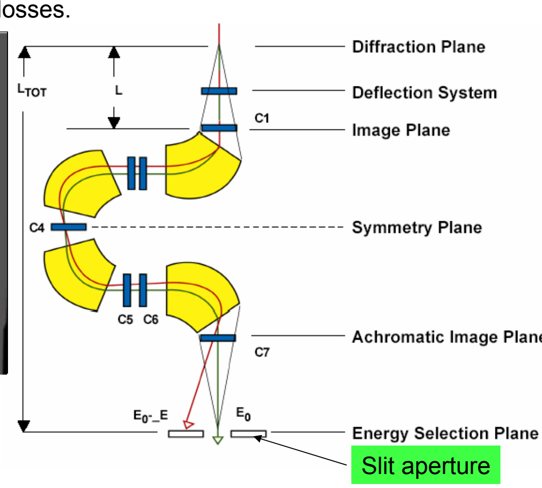

C_1 .. C_7: correction elements

Electron Spectroscopic Imaging (ESI)

Energy-filtered images may also be acquired sequentially by scanning the beam across the specimen and recording a spectrum at every beam position (STEM-EELS).

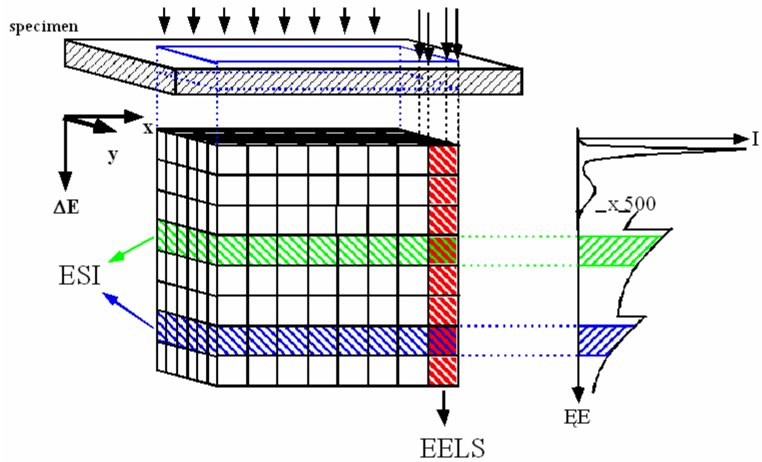

Adding an energy dimension to an image makes it a **3D data cube**

STEM-EELS Maps and Linescans

STEM-EELS:

- Provides a whole spectrum (e.g.1000 .. 4000 energy channels) for each beam position along the scan line (or scanned area)
- Spatial resolution is determined by the electron beam probe size.

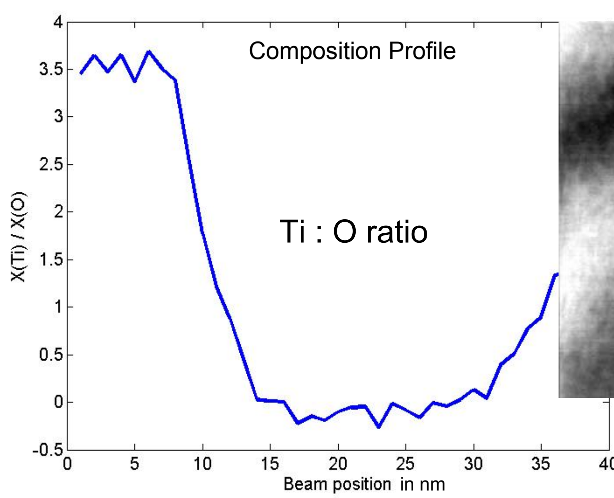

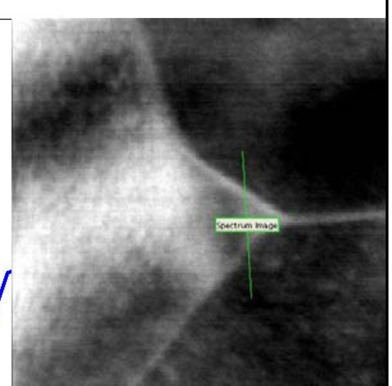

$SrTiO_3$ ceramic

EFTEM vs. STEM-EELS

EFTEM

- Acquisition time independent of number of pixels
- Parallel acquisition ensures zero drift between pixels
- Energy may have shifted between images
- Slit cuts away electrons -> inefficient.

STEM-EELS

- Acquisition time grows linear with number of pixels
- Specimen may have drifted between pixels
- All energy channels acquired simultaneously – no energy drift
- All electrons are used -> very efficient use of electrons

Ionization Edges: Background Subtraction

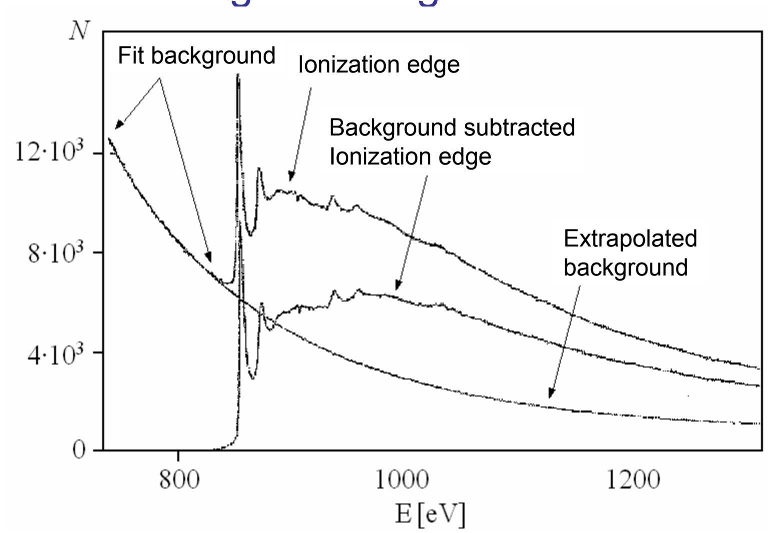

Background extrapolation: usually power law $I_{Background}(E) = AE^{-r}$
(Generally, the background model depends on energy loss)

EFTEM: 3 Window method

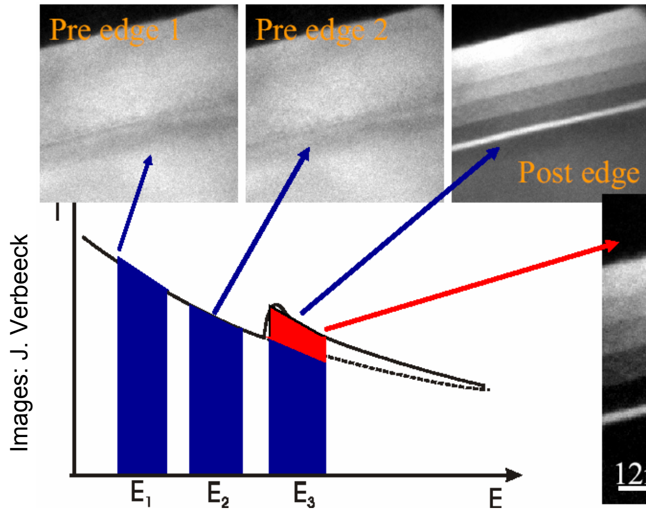

Layered structure $Pr_xCa_{1-x}MnO_3$

Layers with x=1; 0; 0.25; 0.5; 0.75; 1

Substrate $SrTiO_3$

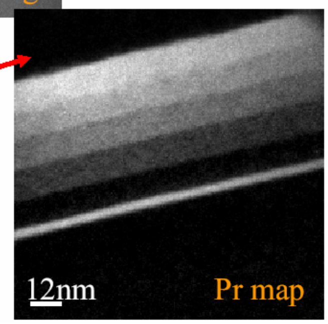

Background extrapolation: usually power law $I_{Background}(E) = AE^{-r}$

Background subtraction in 3-Window Elemental Mapping

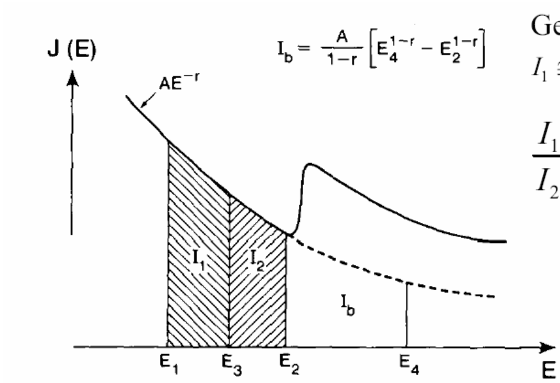

Geometrical average

$$I_1 \cong (E_3 - E_1)[J(E_1)J(E_3)]^{\frac{1}{2}}$$

$$\frac{I_1}{I_2} \approx \frac{E_3 - E_1}{E_2 - E_3}\left[\frac{E_1}{E_2}\right]^{-\frac{r}{2}}$$

$$\frac{I_1}{I_2} \cong \left[\frac{E_2}{E_1}\right]^{-\frac{r}{2}}$$

$$r \cong 2\frac{\log(\frac{I_1}{I_2})}{\log(\frac{E_2}{E_1})}$$

Do this in each pixel - A and r map

It is an approximation

$$A = \frac{(1-r)I_2}{E_2^{1-r} - E_3^{1-r}}$$

From R.F. Egerton

$E_1..E_3$: energies at edge of energy slit

Plasmon Energy Map

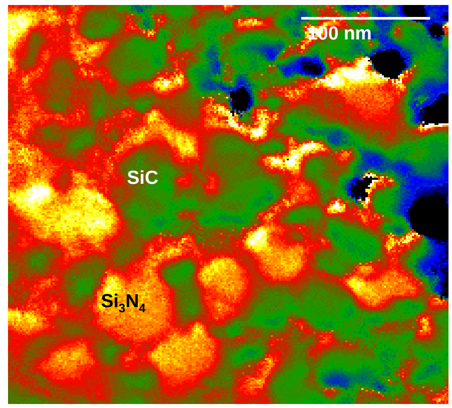

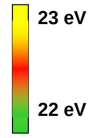

Image: A. Zern, W. Sigle

Map of Plasmon energies in a Si_3N_4 / SiC ceramic determined by fitting the position of the plasmon peak energy to an EFTEM series. The different plasmon energies stem from different **valence electron densities** in these materials. The shift in plasmon energy from left to right is due to an non-isochromaticity of 0.5eV.

Zero-Loss Filtering in Electron Diffraction

Convergent beam electron diffraction (CBED) patterns become much clearer, if the diffuse inelastic scattering background has been removed by zero-loss energy filtering.

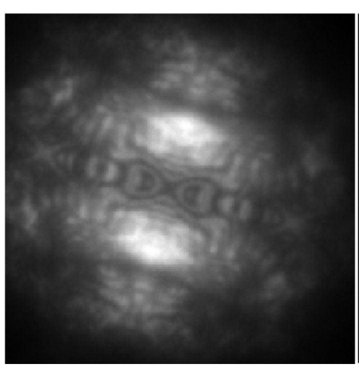

Unfiltered CBED pattern

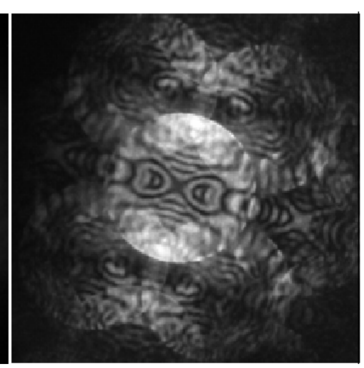

Zero-loss filtered CBED pattern

Image G. Botton

EELS at interfaces

Sequentially acquired EELS Linescan across an interface in Si_3N_4

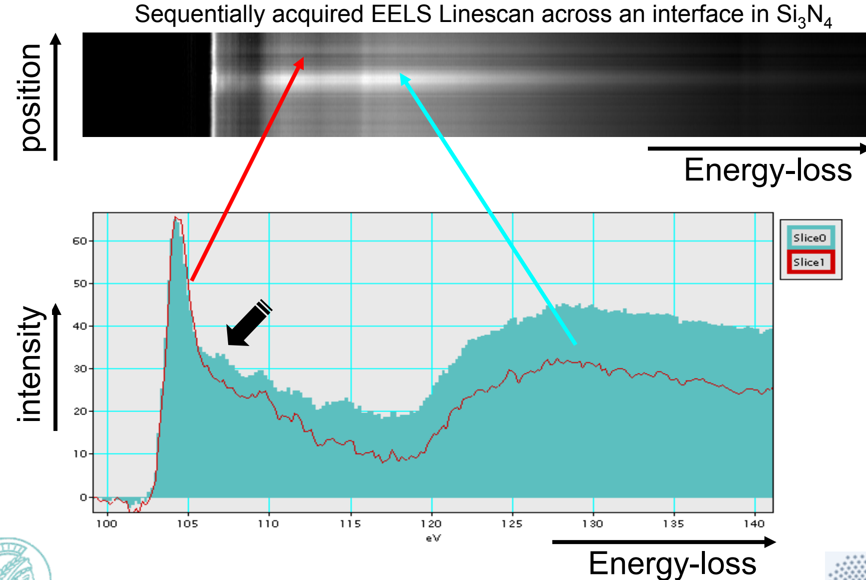

Electron Spectroscopic Profiling (ELSP)

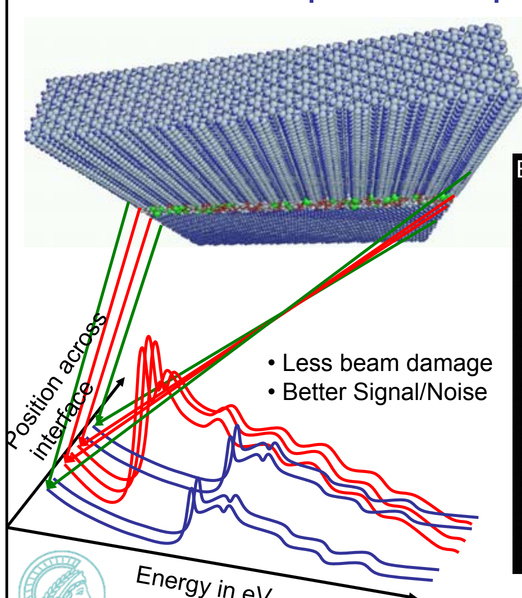

Single focusing spectrometers focus spatial information into a line normal to the dispersive direction.

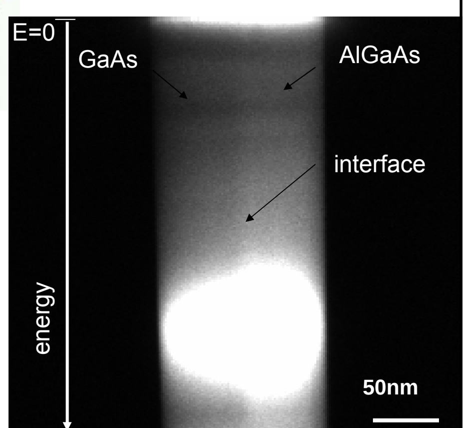

Electron Spectroscopic Profiling (ELSP)

Concentration profiles across an interface from a single exposure!

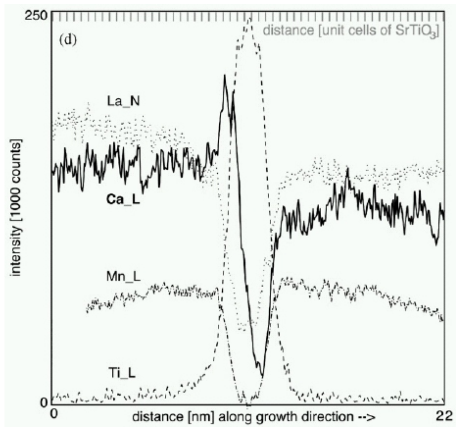

$(La,Ca)MnO_3/SrTiO_3$ – **3.9A resolution**

T. Walther, Ultramicr. **96**, 401 (2003)

EELS at Interfaces

Spatial Difference Technique

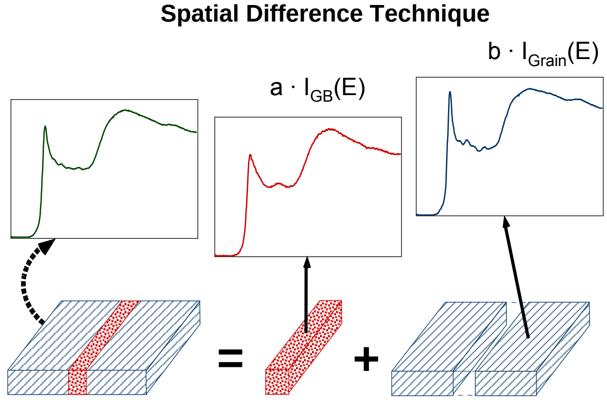

Spectrum incl. interface = a·Spectrum of interface + b·Spectrum of bulk
a + b = 1
each spectrum > 0 at all energies

Momentum-Resolved EELS

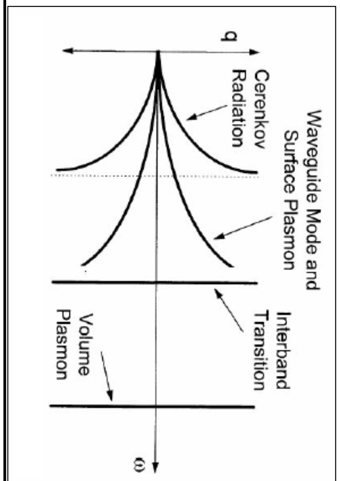

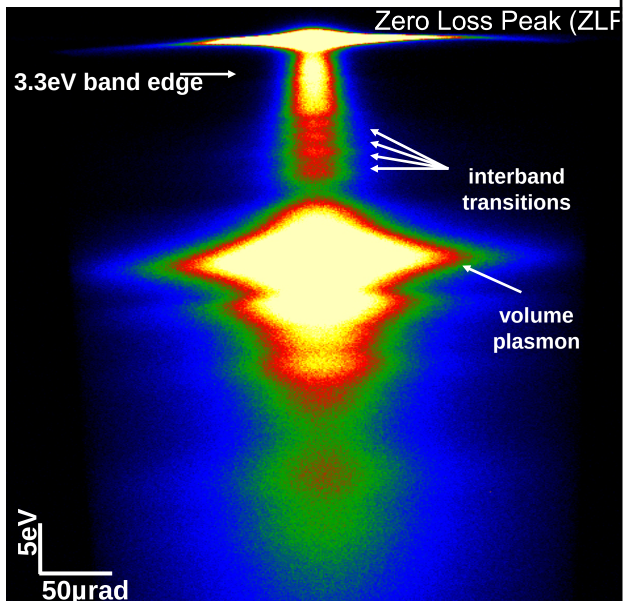

Increasing Energy Resolution: Monochromators

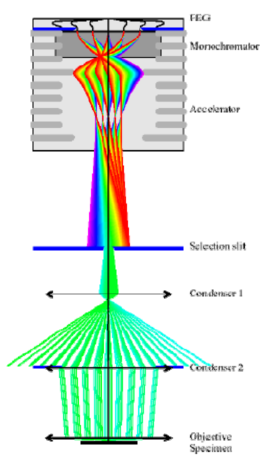

Wien

(has residual dispersion)

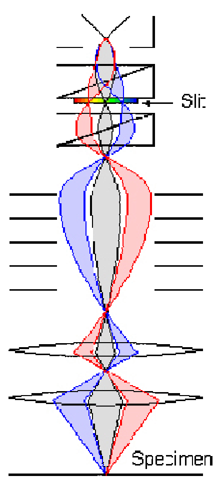

Double Wien

(has residual dispersion)

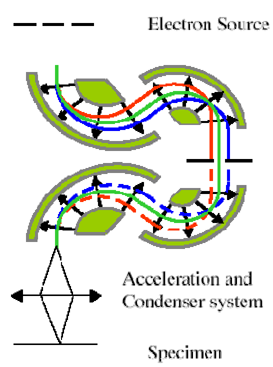

Omega type

(dispersion free)

After Excitation: Relaxation => Characteristic X-rays

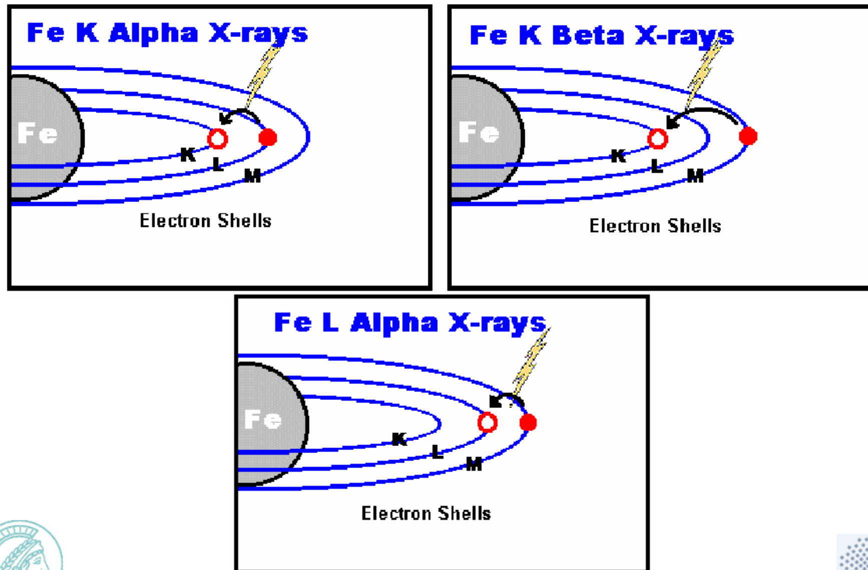

Energy-Dispersive X-ray Spectroscopy (EDXS)

While **EELS probes energy levels of available empty atomic orbitals** into which electrons may be excited (relative to the electron's initial orbital), **EDXS probes the energy levels of filled orbitals** from which electrons may relax to replace the excited electron.

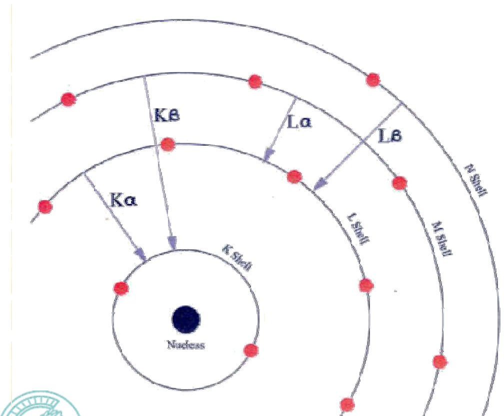

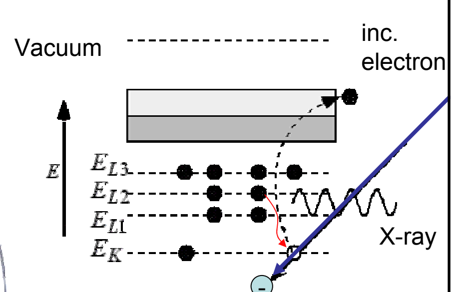

EDXS: Sensitive to Heavy Elements

X-ray emission as function of element (approx.):

$$\omega = \frac{Z^4}{a + Z^4}$$

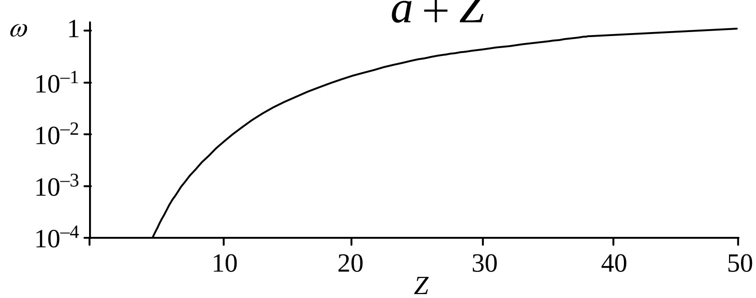

Z: nuclear charge; *a*: constant (e.g. $a \approx 10^6$ for *K*-lines)

Si(Li) - Detector

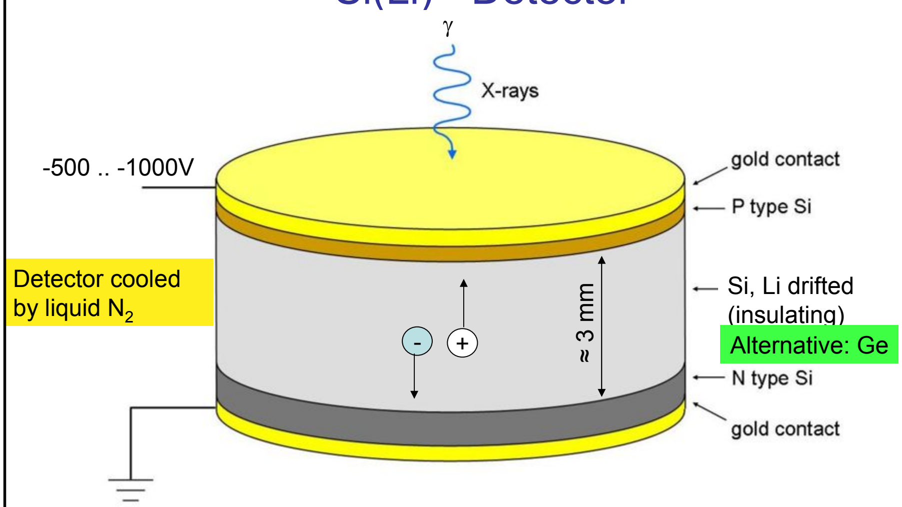

Energy-loss of γ for creating one electron-hole pair: 3.8 eV @ T = 77 K
=> Number of electron-hole pairs proportional to photon-energy (up to a few keV)
charge pulse only ≈ 10^{-16} C (->amplification and computer processing)

Efficiency of Different EDX Detector Designs

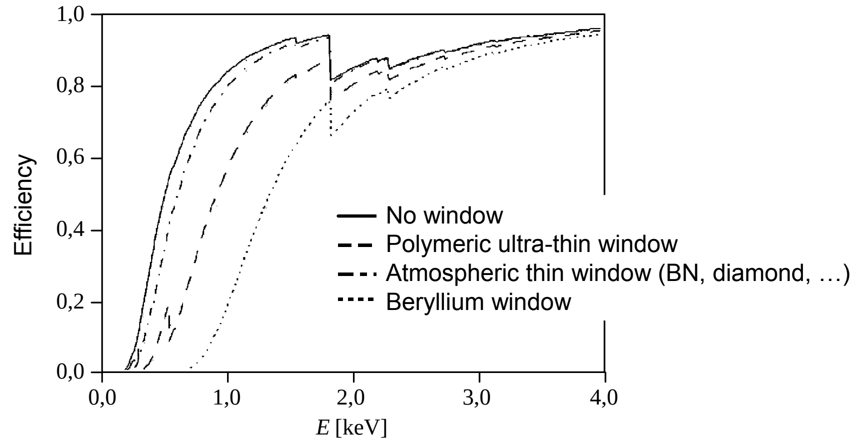

Cooling the detector is necessary, to a) keep the Li in place and b) reduce noise (e.g. thermally activated electron-hole pairs)
Thin windows, transparent to (almost all) X-rays, protect the detector.

EDX Detector

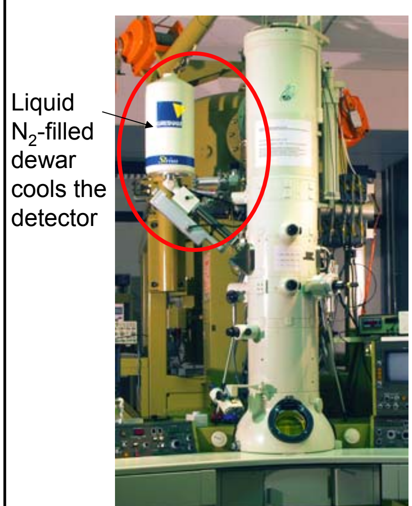

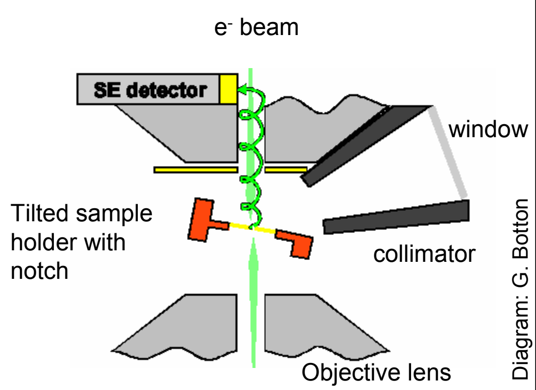

EDX detector

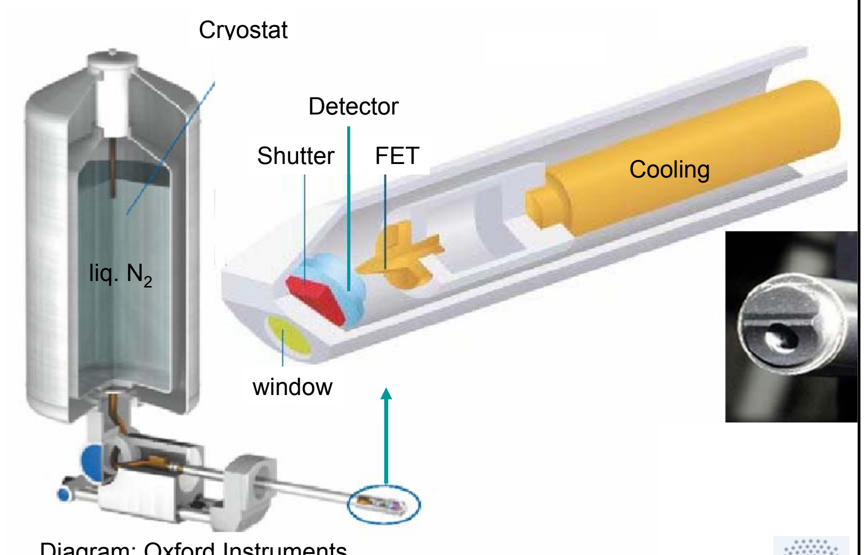

Diagram: Oxford Instruments

The Collimator

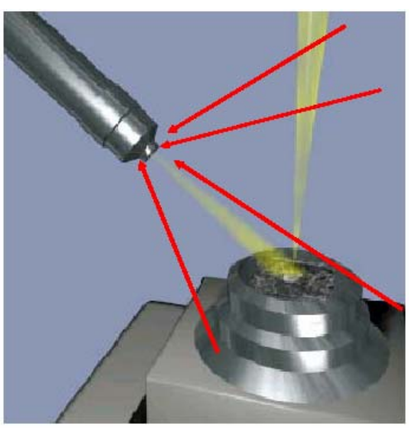

- Collimator - prevents stray radiation entering detector
- Stray radiation can come from secondary excitations any where in the chamber
- Caused by primary x-rays and backscattered electrons hitting chamber components

Diagram: Oxford Instruments
Example: EDX detector in a SEM

The EDX Spectrum

Characteristic X-ray peaks

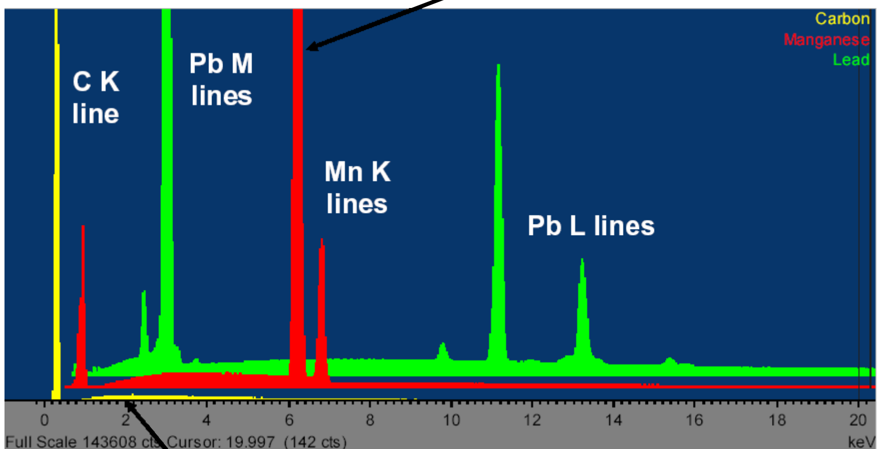

Continuous background (Bremsstrahlung)

EDX mapping of grain junction

BF image

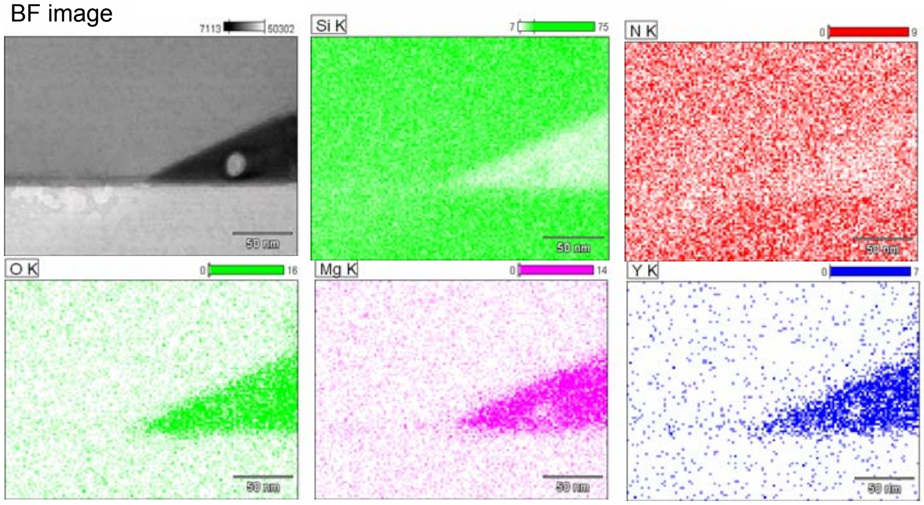

Grain junction in Si_3N_4

Experiment: Z. Zhang

The Inelastic Interaction Volume

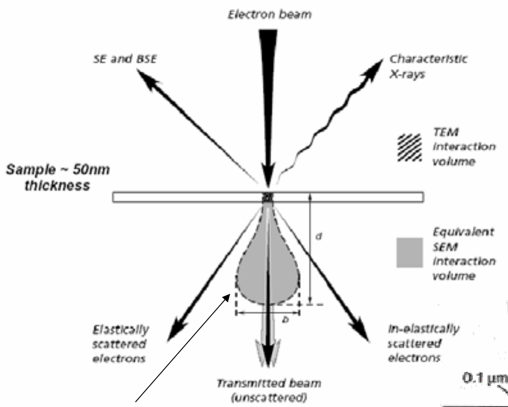

Interaction volume

Because of the **low specimen thickness** the interaction volume in a TEM is much smaller than in SEM. This reduces the count rate, but makes **excellent spatial resolution** possible.

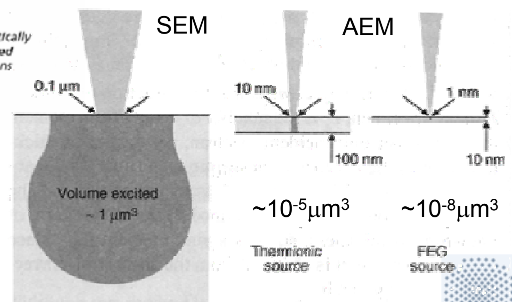

Diagrams: Oxford Instruments

Beam Broadening

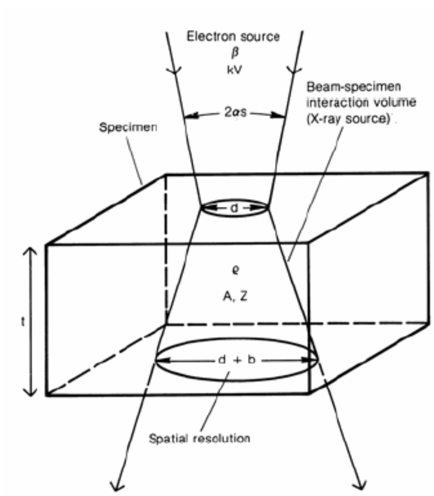

Beam broadening

$$b = 6.25x10^5 \times \left(\frac{Z}{E_0}\right) \times \sqrt{\frac{\rho}{A}} \times t^{3/2}$$

E_0 = Accelerating voltage

z = Atomic number

t = Sample thickness

p = Sample density

A = Atomic weight

Diagram: Oxford Instruments

Spatial Resolution Limit: Specimen Drift

High spatial resolution in EDXS Mapping requires thin specimen and, because of the low count rates, very long exposure times. It then depends on the specimen drift (and the effectiveness of methods compensating it) whether non-blurred EDXS maps can be recorded.

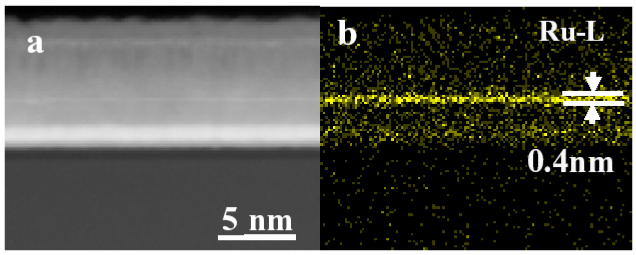

ADF-STEM image   EDX Ru-map

A 4Å thick Ruthenium layer may clearly be resolved by EDXS in a Cs-corrected TEM

Images: T. Yaguchi et al., IMC16 Sapporo, Japan (2006)